Command Governors Based on Bilevel Optimization for Constrained Spacecraft Orbital Transfer

Ilya Kolmanovsky*

University of Michigan, 3038 Francois-Xavier Bagnoud Building, 1320 Beal Avenue, Ann Arbor, MI 48109-2140; ilya@umich.edu

Torbjørn Cunis†

University of Stuttgart, Institute of Flight Mechanics and Control, Pfaffenwaldring 27, Stuttgart, 70569, Germany; tcunis@umich.edu, tcunis@ifr.uni-stuttgart.de

Emanuele Garone[‡]

Université Libre de Bruxelles, Brussels, Belgium; emanuele.garone@ulb.be

The use of Command governors (CGs) to enforce pointwise-in-time state and control constraints by minimally altering reference commands to closed-loop systems has been proposed for a range of aerospace applications. In this paper, we revisit the design of the CG and describe approaches to its implementation based directly on a bilevel (inner loop + outer loop) optimization problem in the formulation of CG. Such approaches do not require offline construction and storage of constraint admissible sets nor the use of online trajectory prediction, and hence can be beneficial in situations when the reference command is high-dimensional and constraints are nonlinear and change with time or are reconfigured online. In the case of linear systems with linear constraints, or in the case of nonlinear systems with linear constraints for which a quadratic Lyapunov function is available, the inner loop optimization problem is explicitly solvable and the bilevel optimization reduces to a single stage optimization. In other cases, a reformulation of the bilevel optimization problem into a mathematical programming problem with equilibrium constraints (MPEC) can be used to arrive at a single stage optimization problem. By applying the bilevel optimization-based CG to the classical low thrust orbital transfer problem, in which the dynamics are represented by Gauss-Variational Equations (GVEs) and the nominal controller is of Lyapunov type, we demonstrate that constraints, such as on the radius of periapsis to avoid planetary collision, on the osculating orbit eccentricity and on the thrust magnitude can be handled. Furthermore, in this case the parameters of the Lyapunov function can be simultaneously optimized online resulting in faster maneuvers.

Nomenclature

r = reference command

v = modified by Command Governor (CG) reference command

x = state

u = control inputw = disturbanceV = Lyapunov function

P = weighting matrix in Lyapunov function

 $\|\cdot\|_2$ = standard Euclidean 2-norm; in the sequel $\|\cdot\| = \|\cdot\|_2$ unless specified otherwise.

Q = weighting matrix in reference governor optimization

 h_i = constraints

 n_c = number of constraints

^{*}Professor, Department of Aerospace Engineering, AIAA Associate Fellow.

[†]Lecturer, Institute of Flight Mechanics and Control; also Adjunct Assistant Research Scientist, Department of Aerospace Engineering, University of Michigan, Member AIAA.

[‡]Professor, Service d'Automatique et Analyse des Systemes, AIAA Senior Member.

 $x_e(v)$ = equilibrium state dependent on v Γ = matrix such that $x_e(v) = \Gamma v$

 ϕ_i = value function of the *i*th inner loop optimization problem

 \mathcal{L} = Lagrangian

 κ = scalar reference governor parameter

a = semi-major axis [km]

e = eccentricity
i = inclination [rad]

 Ω = the Right Ascension of the Ascending node [rad]

 ω = the argument of periapsis [rad] θ = the spacecraft true anomaly [rad]

 r_p = radius of periapsis

 λ_{\min} = minimum eigenvalue of a symmetric matrix λ_{\max} = maximum eigenvalue of a symmetric matrix

 \mathbb{R} = set of real numbers

I. Introduction

REFERENCE governors [1] modify reference commands to nominal closed-loop systems as necessary to enforce pointwise-in-time state and control constraints. The basic schematics of the reference governors are shown in Figure 1. In the variant of the reference governor, referred to as the Command Governor (CG), the reference command is adjusted at discrete-time instants t_k , and the 2-norm difference squared between the original reference command $r_k = r(t_k)$ and modified reference command $v_k = (t_k)$ is minimized subject to the constraint that v_k will not lead to constraint violation if v(t) is maintained at a constant value v_k for all future times. To ensure the latter, one can constrain v_k to a cross section of the sublevel set of a Lyapunov or ISS-Lyapunov function, V, i.e., ensure that $V(v_k, x(t_k)) \le \tilde{c}(v_k)$, where this sublevel set is safe (satisfies the constraints) and is invariant. A simpler implementation [2] is a scalar RG for which $v_k = v_{k-1} + \kappa_k (r_k - v_k)$ and $\kappa_k \in [0, 1]$ is a scalar adjustable parameter.

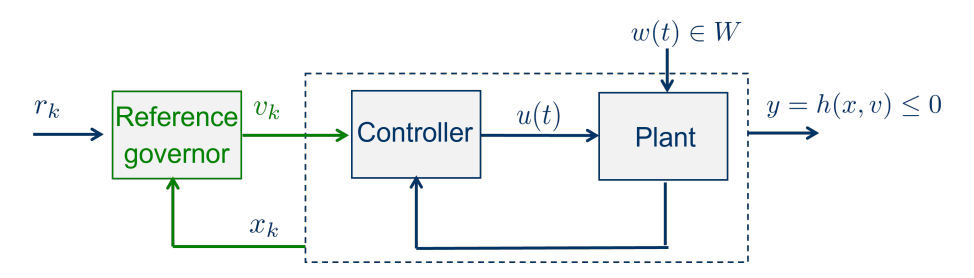


Fig. 1 Reference/Command governor.

In this paper, we consider an approach to implementing the CG without constructing sublevels sets, i.e., $\tilde{c}(\nu)$, offline. This offers advantages in applications where ν is high-dimensional and constraints are nonlinear, in which case generating and storing $\tilde{c}(\nu)$ is not straightforward. An example of such an application is constrained spacecraft orbital transfer where ν corresponds to the commanded values of the semi-major axis, eccentricity, inclination, right ascension of ascending node, and argument of periapsis of the spacecraft and nonlinear constraints are imposed on the orbital elements during the orbital transfer maneuver. Other applications that can potentially benefit from the proposed approach are those where constraints are nonlinear and change or are reconfigured online (see e.g., [3] for a rendezvous and docking case study); in such cases recomputing $\tilde{c}(\nu)$ may not be an option.

In the sequel, we consider a setting where the constraints are imposed in continuous-time while the adjustment of the reference command by the command governor is performed at discrete-time instants.

Our approach is based on bilevel optimization where in the outer loop the normed difference squared between r_k and v_k is minimized subject to the constraints on the value functions of several inner loop optimization problems (each corresponding to an individual constraint). In the case of systems with quadratic Lyapunov functions (typical of the linear system case), and linear constraints, the inner loop optimization problems are explicitly solvable. In a more

general case, a mathematical programming with equilibrium constraints (MPEC) [4] re-formulation of this bilevel optimization problem can be exploited to arrive at a single stage optimization problem which is solved online.

The paper is organized as follows. The background on the conventional RG/CG is briefly reviewed in Section II. Section III considers the bilevel optimization-based CG formulation. Section IV considers the case of linear systems/quadratic Lyapunov functions and linear constraints and derives an explicit formula for the value functions of the inner loop optimization problems, each corresponding to an individual constraint. Systems with the additional unmeasured set-bounded disturbances, $w(t) \in W$, are treated in Section V. Section VI discusses the MPEC reformulation of the CG bilevel optimization problem, which reduces it to a single stage optimization problem with the additional constraints. Several illustrative examples are presented in Section VII and the application to constrained spacecraft orbital transfer based on Gauss Variational Equations (GVEs) is considered in Section VIII.

II. Conventional Command Governor

Consider a closed-loop system represented by the continuous-time nonlinear model of the form,

$$\dot{x} = f(x, v),\tag{1}$$

where x is the state and v is the reference command input altered by CG. The model (1) is specified in continuous-time, and we assume that such a continuous-time model provides a good approximation of the closed-loop system consisting of the nominal system being controlled (plant) and its nominal pre-stabilizing controller which does not handle constraints. The continuous-time treatment of the constraints, as opposed to their discrete-time treatment, is advantageous in addressing inter-sample constraint violation. At the same time, the CG involves online optimization and its updates take place in discrete-time.

The conventional Lyapunov function-based RG/CG [1, 5, 6] relies on the solution of the following optimization problem,

$$J = \frac{1}{2} \| r_k - v \|_Q^2 \to \min_v, \tag{2}$$

subject to

$$V(x_k, v) \le \tilde{c}(v),\tag{3}$$

where x_k is the current state of the system at the time instant t_k (i.e., $x(t_k) = x_k$), r_k is the prescribed reference command, V is a closed-loop Lyapunov function the sublevel sets of which are invariant for constant v, $Q = Q^T > 0$, and $||z||_Q^2 = z^T Qz$ for any z. The value of $\tilde{c}(v)$ is such that

$$V(x_k, v) \le \tilde{c}(v) \Rightarrow h_i(x(t; x(0), v), v) \le 0, \ \forall t \ge t_k, \ i = 1, \dots, n_c,$$

where

$$h_i(x, v) \leq 0$$
,

represents the *i*th scalar constraint that needs to be satisfied and x(t; x(0), v) denotes the solution to (1) corresponding to the initial state x_k at the time instant t_k and with the reference command held at the constaint value, v.

Typically, $\tilde{c}(v)$ is constructed offline and stored for the online use. To construct it, for a given v, either bisections on the value of $\tilde{c}_i(v)$ are performed with $h_i(x, v)$ being maximized with respect to x subject to $V(x, v) \leq \tilde{c}_i(v)$ till the maximum value $h_i^*(v) \approx 0$ or, alternatively, the value of V(x, v) is minimized with respect to x subject to $h_i(x, v) \geq 0$ with $\tilde{c}_i(v)$ set to $V(x^*(v), v)$ where $x^*(v)$ is the minimizer. Then, $\tilde{c}(v) = \min_i \tilde{c}_i(v)$.

If

$$V = \frac{1}{2}(x - \Gamma v)^{\mathsf{T}} P(x - \Gamma v),$$

is quadratic, where $x_e(v) = \Gamma v$ is the equilibrium state corresponding to v, and the *i*th constraint is linear of the form,

$$h_i(x,v) = a_i^\mathsf{T} x + b_i^\mathsf{T} v + c_i \le 0,$$

the explicit formula for $\tilde{c}_i(v)$ is available [7]:

$$\tilde{c}_i(v) = \frac{1}{2} \frac{(h_i(\Gamma v, v))^2}{a_i^{\mathsf{T}} P^{-1} a_i}.$$
(4)

Clearly, (3) can be replaced by a set of constraints

$$V(x_k, v) \le \tilde{c}_i(v), \ i = 1, \dots, n_c, \tag{5}$$

thereby leading to a standard quadratically constrained quadratic programming problem (QCQP) in v given by (2), (4) and (5).

Notably, if constraints are linear and change or are reconfigured online, (4) provides a direct expression for $\tilde{c}_i(v)$. However, such an expression is not available in the more general case in which constraints are nonlinear. Furthermore, (4) only requires constraint values, $h_i(\Gamma v, v)$, $i = 1, \dots, n_c$, in steady-state; these can be determined (mapped) experimentally by slowly varying the reference command to the nominal stabilizing controller if a model for the constraints is not available but distance to constraint violation boundary can be determined.

III. Bilevel optimization problem

An alternative implementation of CG considered in this paper is based on solving the following bilevel optimization problem:

$$J = \frac{1}{2} \| r_k - v \|_Q^2 \to \min_{v}, \tag{6}$$

subject to

$$\phi_i(x_k, v) \le 0, \quad i = 1, \dots, n_c, \tag{7}$$

where $\phi_i(x_k, v)$ is the value function of the inner loop optimization problem,

$$h_i(x, v) \to \max_x$$
 (8)

subject to

$$V(x, v) \le V(x_k, v). \tag{9}$$

Note that x_k is the current state and is known. Implementing CG based on solving the proposed bilevel optimization problem avoids the need to construct and store $\tilde{c}(v)$, which could be nontrivial if v is high-dimensional and n_c is large, or if the constraints change or are reconfigured online.

A large literature on solving bilevel optimization problems exist, see, e.g., [8],[9], [10]. The numerical solution may not be always reliable. It is possible to augment additional acceptance criteria to the numerical solution, v', i.e., conditions under which the assignment $v_k = v'$ is performed; otherwise we use the last value $v_k = v_{k-1}$, feasibility of which is assured by the command governor construction. The acceptance criteria [6] involve checking feasibility of v' (which can be accomplished by forward simulation) and checking the condition,

$$\frac{1}{2}\|v'-r\|_Q^2 \le \frac{1}{2}\|v_{k-1}-r_k\|_Q^2 - \frac{1}{2}\|v'-v_{k-1}\|_Q^2.$$
(10)

which ensures convergence to constant set-points [6].

IV. Linear Systems/Quadratic Lyapunov Functions and Linear Constraints

Suppose that the *i*th scalar constraint has the form,

$$h_i(x, v) = a_i^{\mathsf{T}} x + b_i^{\mathsf{T}} v + c_i \le 0,$$
 (11)

and the Lyapunov function is given by

$$V(x, v) = \frac{1}{2}(x - \Gamma v)^{\mathsf{T}} P(x - \Gamma v),$$

where $P = P^{\mathsf{T}} > 0$ and $x_e(v) = \Gamma v$ is the equilibrium state corresponding to v. Assuming $x_k \neq \Gamma v$ (otherwise, $x = \Gamma v$ is the solution to (8)-(9)), Slater's constraint qualification condition holds and Karush-Kuhn-Tucker (KKT) conditions can be applied to determine solutions to the inner-loop optimization problem (8)-(9)). The Lagrangian has the form,

$$\mathcal{L} = -a_i^\mathsf{T} x - b_i^\mathsf{T} v - c_i + \lambda_i \left(\frac{1}{2} (x - \Gamma v)^\mathsf{T} P(x - \Gamma v) - \frac{1}{2} (x_k - \Gamma v)^\mathsf{T} P(x_k - \Gamma v) \right),$$

where $\lambda_i \in \mathbb{R}$ designates the Lagrange multiplier. The stationarity condition leads to

$$\lambda_i P(x - \Gamma v) = a_i \Rightarrow x = \Gamma v + \lambda_i^{-1} P^{-1} a_i$$
.

As the constraint is active at the minimizer,

$$\frac{1}{2}a_i^{\mathsf{T}}\frac{1}{\lambda_i^2}P^{-1}a_i = V(x_k,v) \Rightarrow \lambda_i^{-1} = \sqrt{\frac{2V(x_k,v)}{a_i^{\mathsf{T}}P^{-1}a_i}},$$

and

$$x = \Gamma v + \sqrt{\frac{2V(x_k, v)}{(a_i^\intercal P^{-1} a_i)}} P^{-1} a_i.$$

Hence,

$$\phi_i(x_k, v) = a_i^{\mathsf{T}} \Gamma v + \sqrt{2V(x_k, v)} \sqrt{(a_i^{\mathsf{T}} P^{-1} a_i)} + b_i^{\mathsf{T}} v + c_i.$$
 (12)

Note that (12) holds also if $x_k = \Gamma v$, in which case $V(x_k, v) = 0$, and $x = \Gamma v$ is the solution.

Thus the inner loop optimization problem (8)-(9)) is explicitly solvable, and the outer loop optimization problem becomes

$$J = \frac{1}{2} \| r_k - v \|_Q^2 \to \min_{v}, \tag{13}$$

subject to

$$\phi_i(x_k, v) \le 0, \quad i = 1, \dots, n_c, \tag{14}$$

where $\phi_i(x_k, v)$, $i = 1, \dots, n_c$, are given by the explicit expressions above and x_k is the current state, which is known. Note that the function ϕ_i in (12) is convex, Lipschitz continuous and is differentiable everywhere except at $v = \Gamma x_k$, where the latter is the case in steady-state. The gradients are given by

$$\nabla_{v}\{J\} = Q(v - r_k), \quad \nabla_{v}\{\phi_i(x_k, v)\} = \Gamma^\mathsf{T} a_i + b_i + \frac{\sqrt{(a_i^\mathsf{T} P^{-1} a_i)} \Gamma^\mathsf{T} P(\Gamma v - x_k)}{\sqrt{2V(x_k, v)}}.$$

If a scalar reference governor strategy is implemented in which $v = v_{k-1} + \kappa(r - v_{k-1})$, $\kappa \in [0, 1]$, then the optimization problem can be solved by the standard bisections in the scalar variable κ , requiring no differentiability. Otherwise, either conventional gradient-based optimizers (in a heuristic manner given almost everywhere differentiability), nonsmooth optimizers [11] or derivative-free optimizers such as genetic algorithms [9] could be employed.

As another alternative, the problem can be approximated by the standard quadratic program (QP) with extra constraints and variables. Let matrix S and vector s define a polyhedron inscribed into the unit 2-norm ball with the origin in the interior, i.e., $Sz \le s$ implies $||z||_2 \le 1$, where s > 0. Then the QP (with all constraints being linear) takes the following form:

$$J = \frac{1}{2} \| r_k - v \|_Q^2 \to \min_{v, \alpha_i, i=1, \dots, n_c},$$
(15)

subject to

$$SP^{\frac{1}{2}}(x_k - \Gamma v) - s\alpha_i \leq 0,$$

$$-\alpha_i \leq 0,$$

$$\alpha_i \sqrt{(a_i^{\mathsf{T}}P^{-1}a_i)} + a_i^{\mathsf{T}}\Gamma v + b_i^{\mathsf{T}}v + c_i \leq 0, i - 1, \dots, n_c,$$

$$Correction 1 change "-" to "=" in equation (18) so that i=1, \cdot cdots, n_c (17)$$

$$(17)$$

where α_i , $i=1,\cdots,n_c$ are treated as extra variables in the optimization. Indeed, for any feasible solution to the above QP, $\alpha_i \ge 0$, $i=1,\cdots,n_c$. Let $z=P^{\frac{1}{2}}(x_k-\Gamma v)$, then $\sqrt{2V(x_k,v)}=\|z\|$ and, by (16), $\|z\| \le \alpha_i$ for all $i=1,\cdots,n_c$, implying

$$\phi_i(x_k,v) = a_i^\mathsf{T} \Gamma v + \sqrt{2V(x_k,v)} \sqrt{(a_i^\mathsf{T} P^{-1} a_i)} + b_i^\mathsf{T} v + c_i \leq a_i^\mathsf{T} \Gamma v + \alpha_i \sqrt{(a_i^\mathsf{T} P^{-1} a_i)} + b_i^\mathsf{T} v + c_i \leq 0.$$

Thus v_k chosen according to the solution of QP (15)-(18) will guarantee feasibility and no constraint violation. However, recursive feasibility of this QP is not guaranteed. Hence acceptance/rejection logic discussed at the end of Section III should be used.

V. Systems with Disturbances

In the case of systems with set-bounded unmeasured disturbances, $w(t) \in W$, for all $t \ge 0$, CG implementation can be based on Input-to-State Stable (ISS) Lyapunov functions, V(x, v), for which suffuciently large sized sublevel sets remain invariant despite the disturbances. Specifically, suppose the system is time-invariant and the property,

$$V(x(0), v) \ge \gamma(v) \Rightarrow V(x(t; x(0), w(\cdot), v), v) \le V(x(0), v), \forall t \ge 0, \forall w(\cdot \in W, (19))$$

is satisfied where $x(t; x(0), w(\cdot), v), v)$ is the solution corresponding to x(0), the disturbance $w(\cdot)$ with $w(t) \in W$ for all $t \ge 0$, and constant v. In this case, in the inner loop of the bilevel optimization problem, equations (8)-(9) are replaced by

$$h_i(x, v) \to \max_x$$
 (20)

subject to

$$V(x, v) \le \bar{V}(x_k, v) := \max\{V(x_k, v), \gamma(v)\}.$$
 (21)

In the case of linear systems with linear constraints in Section IV, the only change necessary is in equation (12) which is modified to

$$\phi_i(x_k, v) = a_i^{\mathsf{T}} \Gamma v + \sqrt{2\bar{V}(x_k, v)} \sqrt{(a_i^{\mathsf{T}} P^{-1} a_i)} + b_i^{\mathsf{T}} v + c_i.$$
 (22)

Finally, assuming the dynamics are given by $\dot{x} = Ax + Bv + B_1w$, $w \in W$, and the ISS-Lyapunov function has the form, $V(x) = \frac{1}{2}(x - \Gamma v)^{\mathsf{T}}P(x - \Gamma v)$, $A^{\mathsf{T}}P + PA + \bar{Q} = 0$, and $\bar{q} > 0$, the computation of $\gamma(v)$ in (21) reduces to

$$\gamma(v) = \frac{1}{2\bar{q}} \frac{\lambda_{\max}(P)}{\lambda_{\min}(\bar{Q} - \bar{q}P)} \max_{w \in W} w^{\mathsf{T}} B_1^{\mathsf{T}} P B_1 w, \tag{23}$$

where $\lambda_{\min}(\cdot)$ and $\lambda_{\max}(\cdot)$ denote the minimum and maximum eigenvalues of a symmetric matrix.

VI. MPEC Reformulation

One of the strategies for solving the bilevel optimization problem is through the mathematical programming with the equilibrium constraints (MPEC), see e.g., [8], in which the inner-loop optimization problem is replaced by first-order necessary conditions. The MPEC-based reformulation of the bilevel optimization problem in Section III has the following form:

$$J = \frac{1}{2} \| r_k - v \|_Q^2 \to \min_{v \in \bar{I}, \bar{v}}$$
 (24)

subject to

$$h_i(x^{(i)}, v) \le 0, \ i = 1, \dots, n_c,$$
 (25)

$$-\nabla_x h(x^{(i)}, v) + \lambda^{(i)} \nabla_x V(x^{(i)}, v) = 0$$
(26)

$$\lambda^{(i)}(V(x^{(i)}, v) - V(x_k, v)) = 0, (27)$$

$$-\bar{\lambda} \le 0,\tag{28}$$

where $v, \bar{x} = (x^{(1)}, \dots, x^{(n_c)}), v$ and the vector of Lagrange multipliers, $\bar{\lambda} = (\lambda^{(1)}, \dots, \lambda^{(n_c)})$ are optimized variables. Note that if $h_i(x, v)$ is convex as a function of x and sublevel sets of V are convex, then the maximum in (8)-(9) is reached on the boundary, and the complementarity constraint (27) can be replaced by an equality constraint,

$$V(x^{(i)}, v) = V(x_k, v).$$
 (29)

On the other hand, in the case when $h_i(x, v)$ is concave as a function of x, the necessary conditions (25)-(28) are sufficient conditions; thus arriving at a solution of (25)-(28) ensures that a maximizer of the inner loop optimization problem is obtained.

In general, the optimization problem (24)-(28) has to be solved numerically. The case of a linear model with linear constraints is an exception as in this case the inner loop optimization problem can be solved explicitly (see Section IV).

VII. Illustrative Examples

A. Example 1

As an example, suppose the nominal closed-loop system dynamics are given by

$$\dot{x} = Ax + B(v + w),$$

where

$$A = \begin{bmatrix} 0 & 1 \\ -\omega_n^2 & -2\zeta\omega_n \end{bmatrix}, \quad B = \begin{bmatrix} 0 \\ \omega_n^2 \end{bmatrix},$$

 $\omega_n = 3$, $\zeta = 0.2$. We set $\Gamma = \begin{bmatrix} 1 & 0 \end{bmatrix}^\mathsf{T}$ and find P by solving the Lyapunov equation, $A^\mathsf{T}P + PA = -I$. We set Q = 1 in the CG implementation and impose the state constraints as $x \in [-1, 1] \times [-1.3, 1.3]$. This corresponds to $n_c = 4$ constraint functions h and hence four different constraints $\phi_i(x_k, v) \leq 0$ of the form (12) corresponding to the four choices of values of a, b, c.

The CG updates the reference every $\Delta T = 0.1$ sec, while continuous-time dynamics are propagated between the update time instants. We use fmincon in Matlab to solve the optimization problem (13)-(14) with ϕ_i given by (22), leaving the application of nonsmooth optimization numerical algorithms [11] to future work.

The response with no disturbance ($W = \{0\}$) is shown in Figure 2. The response with the disturbance confined to the set W = [-0.015, 0.015] is shown in Figure 3. In the latter case, with $\bar{q} = 0.1$, $\gamma(v) = 0.3098$ and is independent of v. Note that CG is significantly more conservative in the case with the disturbance, but in both cases with and without disturbances avoids constraint violations. The simulated disturbance for the trajectories shown in Fig. 3 is given by $w(t) = 0.015 \text{sign}(\sin(4\pi\omega_n t))$.

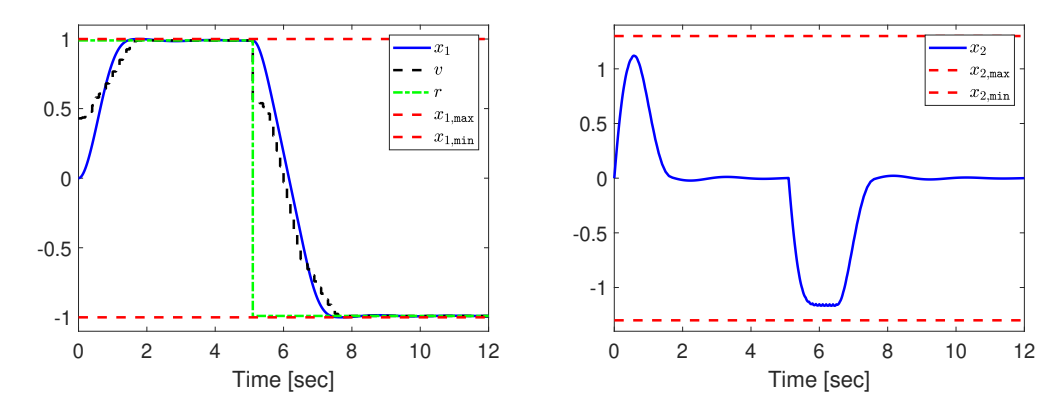


Fig. 2 Left: Time histories of x_1 , v, r and constraints in Example 1 with no disturbance. Right: Time histories of x_2 , and constraints in Example 1 with no disturbance.

B. Example 2

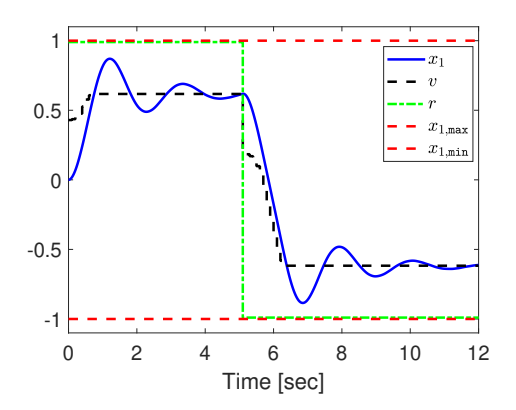
As another example, suppose the nominal closed-loop system dynamics are given by

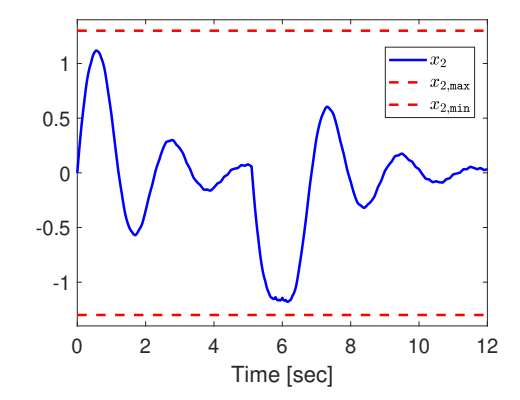
$$\dot{x} = Ax + Bv,$$

where

$$A = \begin{bmatrix} 0 & 1 & 0 & 0 \\ -\omega_{n,1}^2 & -2\zeta_1\omega_{n,1} & 0 & 0 \\ 0 & 0 & 0 & 1 \\ 0 & 0 & -\omega_{n,2}^2 & -2\zeta_2\omega_{n,2} \end{bmatrix}, \quad B = \begin{bmatrix} 0 & 0 \\ \omega_{n,1}^2 & 0 \\ 0 & 0 \\ 0 & \omega_{n,2}^2 \end{bmatrix},$$

 $\omega_{n,1} = 5$, $\zeta_1 = 0.01$, $\omega_{n,2} = 2$, $\zeta_2 = 0.02$. These equations describe the motion on the x_1 - x_3 plane driven by two independent mass-spring-damper systems along each axis. The system is lightly damped.





add after equation for $x \in (v)$ on top of

Fig. 3 Left: Time histories of x_1 , v, r and constraints in Example 1 with disturbance. Right: Time histories of x_2 and constraints in Example 1 with disturbance.

We let $x_{e,1}(v) = -r_0 \cos v$, $x_{e,3}(v) = r_0 \sin v$ and

$$\Gamma = \begin{bmatrix} 1 & 0 \\ 0 & 0 \\ 0 & 1 \\ 0 & 0 \end{bmatrix}, \quad x_e(v) = \Gamma \begin{bmatrix} x_{e,1}(v) \\ x_{e,3}(v) \end{bmatrix}, \quad u = [x_{e,1}(v)],$$

$$u = [x_{e,3}(v)],$$

so that $x_e(v)$ is the steady-state equilibrium corresponding to v. We find P by solving the Lyapunov equation, $A^TP + PA = -I$ and define the Lyapunov function as

$$V(x, v) = \frac{1}{2}(x - x_e(v))^{\mathsf{T}} P(x - x_e(v)).$$

We impose the state constraints as

$$h_1(x) = -x_1^2 - x_3^2 + r_l^2 \le 0, \quad h_2(x) = x_1^2 + x_3^2 - r_u^2 \le 0,$$

where $r_u > r_0 > r_l > 0$. This corresponds to $n_c = 2$ constraint functions h which are nonlinear. We choose $r_u = 3$, $r_0 = 2$, $r_l = 1$.

The reference governor updates the reference every $\Delta T = 0.1$ sec, while continuous-time dynamics are propagated between the update time instants. We use fmincon to solve MPEC problem (24), (25), (26), (28) and (29) numerically. Given that h_2 is not concave, we use the acceptance logic (10) to enhance the reliability of the solution.

The response is shown in Figures 4-5. All the constraints are enforced and the modified reference command converges to the desired reference command in finite time whenever the desired reference command remains constant.

C. Example 3

We now take $\omega_{n,1} = \sqrt{15}$, $\zeta_1 = 0.005$, $\omega_{n,2} = 2$, $\zeta_2 = 0.02$ in Example 2, and change the constraints to $h_1(x) = -x_1^2 - x_3^2 + r_1^2 \le 0$, $h_2(x) = -x_1^2 - (x_3 - 5.5)^2 + r_u^2 \le 0$,

where $r_l = 1$, $r_u = 3$, $r_0 = 1$. Note that both constraints are concave and so in this case the necessary conditions for the inner loop optimization problems are also sufficient. The response is shown in Figures 6-7. All constraints are enforced and the modified reference command by CG converges to the desired reference command in finite time whenever the desired reference command remains constant.

VIII. Orbital Transfers

The spacecraft orbit and its position in the orbit can be characterized by the orbital elements which are the semi-major axis a [km], the eccentricity e, the inclination i [rad], the Right Ascension of the Ascending node Ω [rad], the argument of periapsis ω [rad] and the spacecraft true anomaly θ [rad]. See Figure 8.

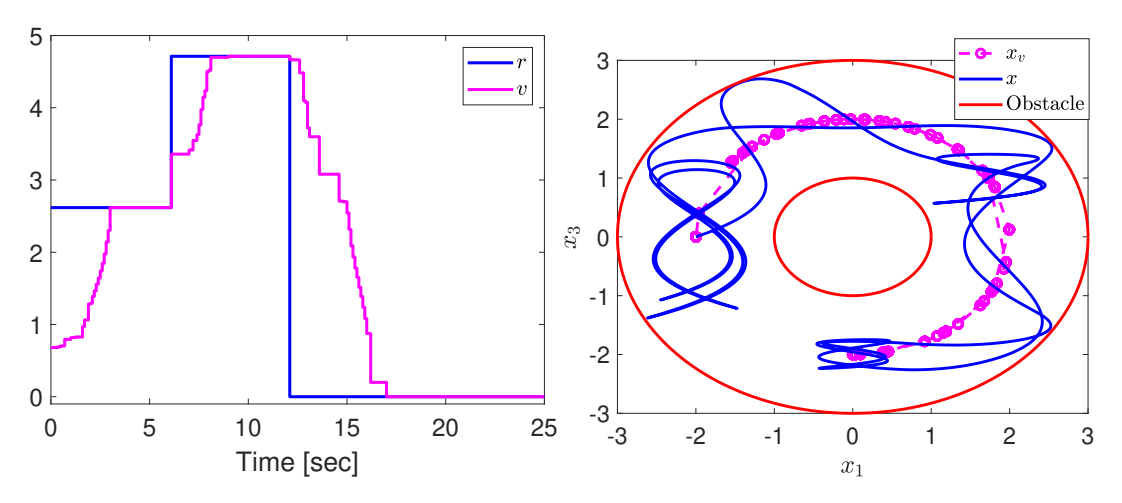


Fig. 4 Left: Time histories of v, r in Example 2. Right: Trajectory on x_1 - x_3 plane of the actual x, $x_e(v)$ and constraints in Example 2.

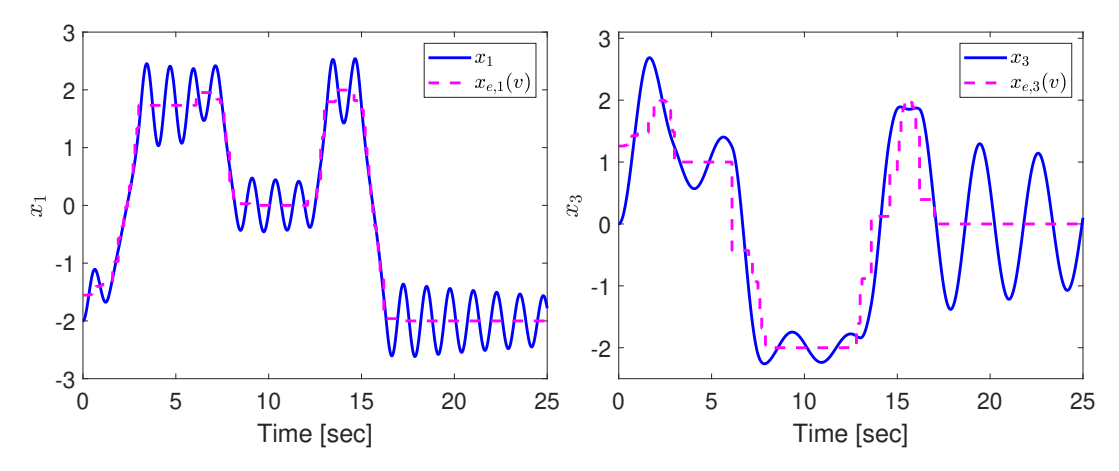


Fig. 5 Left: Time history of x_1 and $x_{e,1}(v)$ in Example 2. Right: Time history of x_3 and $x_{e,3}(v)$ in Example 2.

The Gauss Variational Equations (GVEs) describe the evolution of the orbital elements of the spacecraft and are given by [12, 13]:

$$\frac{da}{dt} = \frac{2a^2}{\sqrt{\mu p}} e \sin \theta S + \frac{2a^2}{\sqrt{\mu p}} \frac{p}{r} T,$$

$$\frac{de}{dt} = \frac{p \sin \theta}{\sqrt{\mu p}} S + \frac{p(\cos \psi + \cos \theta)}{\sqrt{\mu p}} T,$$

$$\frac{di}{dt} = \frac{r}{\sqrt{\mu p}} \cos (\theta + \omega) W,$$

$$\frac{d\Omega}{dt} = \frac{r}{\sqrt{\mu p}} \frac{\sin (\theta + \omega)}{\sin i} W,$$

$$\frac{d\omega}{dt} = -\frac{p \cos \theta}{e \sqrt{\mu p}} S + \frac{(r + p) \sin \theta}{e \sqrt{\mu p}} T - \frac{r \sin(\theta + \omega) \cot i}{\sqrt{\mu p}} W,$$

$$\frac{d\theta}{dt} = \frac{\sqrt{\mu p}}{r^2} + \frac{p \cos \theta}{e} \frac{S}{\sqrt{\mu p}} - \frac{p + r}{e} \cos \theta \frac{T}{\sqrt{\mu p}},$$
(30)

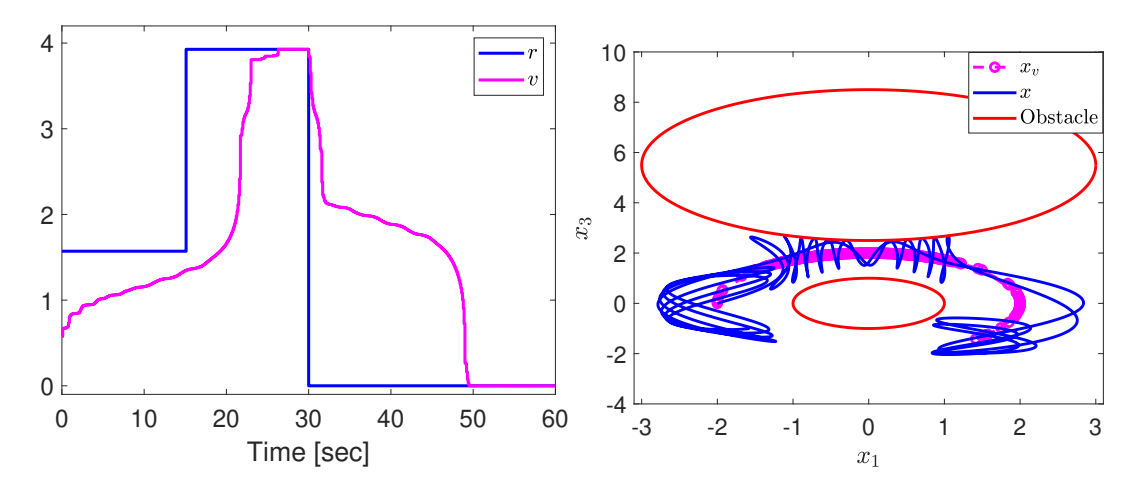


Fig. 6 Left: Time histories of v, r in Example 3. Right: Trajectory on x_1 - x_3 plane of the actual x, $x_e(v)$ and constraints in Example 3.

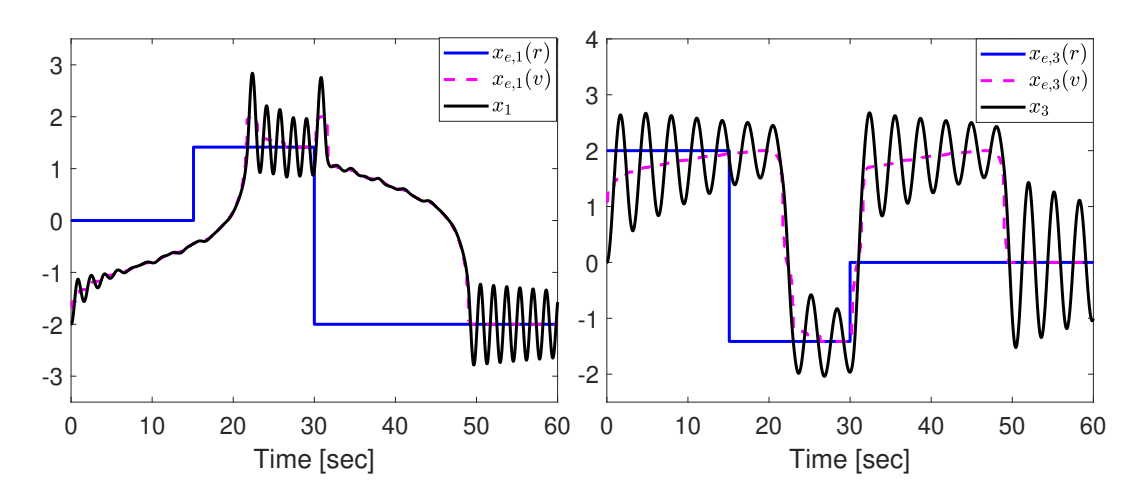


Fig. 7 Left: Time history of x_1 and $x_{e,1}(v)$ in Example 3. Right: Time history of x_3 and $x_{e,3}(v)$ in Example 3.

where $r = \frac{p}{1+e\cos\theta}$ is the distance from the gravity center to the spacecraft center of mass*, $p = a(1-e^2)$ is the orbit parameter, and $\psi = \arccos\left(\frac{1}{e} - \frac{r}{ae}\right)$ is the eccentric anomaly. The S,T and W are the components of the thrust-induced relative acceleration [km/s²] in the S-T-W frame.

Let

$$x = [a \ e \ i \ \Omega \ \omega]^{\mathsf{T}}, \ u = [S \ T \ W]^{\mathsf{T}}.$$

Then the first five of GVEs (30) can be written in the following condensed form:

$$\dot{x}(t) = G(x(t), \theta(t))u(t), \tag{31}$$

where $G(x(t), \theta(t)) \in \mathbb{R}^{5\times 3}$. Note that since the objective is to steer the spacecraft into a target orbit but not to a particular location in that orbit (each location will be visited due to periodicity of the orbit) the true anomaly $\theta(t)$ is not included into the state vector x(t) and is treated as a time-varying parameter the evolution of which is determined by the sixth equation in (30).

^{*}We use r to denote the distance to the gravity center in this section to be consistent with the standard notation used in astrodynamics, and we use x_{des} to denote the vector of target orbital elements (reference command).

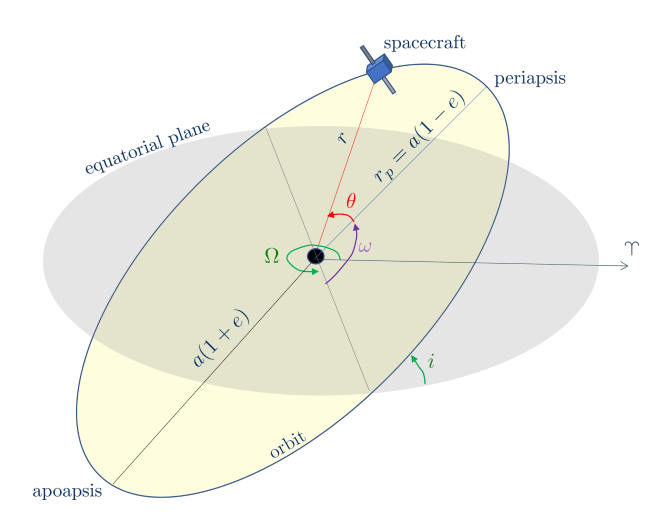


Fig. 8 Classical orbital elements.

Three constraints are considered on the spacecraft trajectory during the orbital transfer:

$$h_1(x) = -a(1-e) + r_{\min} \le 0,$$
 (32)

$$h_2(x, \nu, \theta) = -u_{\max}^2 + \|u\|_2^2 \le 0, (33)$$

and

$$h_3(x) = -e + e_{\min} \le 0. {34}$$

The first constraint (32) is imposed to ensure that the radius of the periapsis of the osculating orbit is always above the minimum allowed value of r_{\min} . This constraint ensures that the spacecraft collision with the primary body is avoided even in the event of thrust failures (as a result of which thrust becomes zero). The second constraint (33) ensures that the thrust magnitude limits are not exceeded. The third constraint (34) limits the eccentricity to the value above e_{\min} to maintain the model in the validity range.

To achieve tracking, while satisfying the constraints (32) and (34), consider a Lyapunov function candidate,

$$V(x, \nu, P) = \frac{1}{2}(x - \nu)^{\mathsf{T}} P(x - \nu), \tag{35}$$

where $P = P^{\mathsf{T}} > 0$ is a 5×5 positive-definite weight matrix. The time derivative of V(x(t), v, P) along the trajectories of (31) and assuming v and P remain constant in-time is given by

$$\frac{d}{dt}V(x(t), v, P) = (x(t) - v)^{\mathsf{T}}PG(x(t), \theta(t))u(t)$$
(36)

Let

$$u_{\text{nom}}(x, v, \theta) = -(x - v)^{\mathsf{T}} PG(x, \theta). \tag{37}$$

To enforce the control constraints (33), we simply project $u_{\text{nom}}(x, v, \theta)$ on the feasible set of control values so that

$$u(t) = \begin{cases} u_{\text{nom}}(t), & \text{if } ||u_{\text{nom}}(t)|| \le u_{\text{max}}, \\ \frac{u_{\text{nom}}(t)}{||u_{\text{nom}}(t)||} u_{\text{max}}, & \text{otherwise,} \end{cases}$$
(38)

From (36), (37), (38) and given that u(t) is a 2-norm projection of $u_{nom}(t)$ on the ball of radius u_{max} in \mathbb{R}^3 it follows that

$$\dot{V} = -(x - v)^{\mathsf{T}} PG(x, \theta) u(t) \le -u_{\mathsf{nom}}^{\mathsf{T}}(t) u(t) \le -u^{\mathsf{T}}(t) u(t) \le 0,$$

implying that the sub-level sets of V are positively invariant (for constant in time v and P).

The constraint (32) is nonlinear. We illustrate handling it, along with (34) using the procedure in Section IV. For this, we firstly approximate (32) by a piecewise linear function, $\tilde{h}_1(x) = \min_j \{x : h_{1,j}(x) \le 0\}$, where $h_{1,j}$, $j = 1, \dots, 9$,

are affine functions so that $h_1(x) \le \tilde{h}_1(x)$ for all x and we replace (32) by $\tilde{h}_1(x) \le 0$ which decomposes into the set of linear inequality constraints, $h_{1,j}(x) \le 0$, $j = 1, \dots, 9$.

We can now compute v_k using the procedure in Section IV, applied to $h_{1,j}$, $j = 1, \dots, 9$, h_3 , and $\Gamma = I$ while noting that h_2 is enforced due to (38). We do this with an additional enhancement based on the observation that (35) is a closed-loop Lyapunov function for any choice of P > 0. Given that the constraint (32) constrains only the two orbital elements, a and e, we set

$$P = P(z_1, z_2) = diag([7.5 \times 10^{-11}z_1, 0.0100z_2, 0.0050, 0.0075, 0.0005]),$$
(39)

where z_1 , z_2 are treated as the additional optimization variables satisfying the constraints, $0.5 \le z_1 \le 2$, $0.5 \le z_2 \le 2$. We set $Q = diag([7.5 \times 10^{-11}, 0.0100, 0.0050, 0.0075, 0.0005]) = <math>P(1, 1)$ in (13) and solve the problem (13)-(14) with the additional variables z_1 and z_2 numerically using fmincon and without the acceptance logic (10). Thus the proposed scheme combines features of a CG and a parameter governor of [14]. The updates of v_k and of $z_{1,k}$, $z_{2,k}$ occur every $\Delta T = 1$ hour.

Simulation results are now reported. Firstly, without CG the constraints can be violated. For example, Figure 9 illustrates the transfer from a higher earth orbit to a lower earth orbit, corresponding to

$$x(0) = \begin{bmatrix} 21378, \ 0.7, \ \frac{\pi}{10}, \ 0, \ \pi \end{bmatrix}^\mathsf{T}, \ \theta(0) = \pi,$$
Correction 3: Add after equation (41) and the value of r_{min} , the value of

and desired final conditions corresponding to the target orbit,

$$x_{\text{des}} = \left[6878, \ 0.02, \ \frac{\pi}{2}, \ \frac{3\pi}{2}, \ \pi \right]^{\mathsf{T}} = \left[\frac{\exp\{\min\} = 10^{-3}\}}{2} \right]$$
 (41)

In the simulations, $\mu = 398600.4405 \text{ km}^3/\text{s}^2$, $r_{\text{min}} = 6628 \text{ km}$, and the thrust constraints (33) are imposed with $u_{\text{max}} = 0.001 \text{ kN/kg}$. The constraint (32) is violated implying that in the event of spacecraft thruster failure, $r(t) < r_{\text{min}}$ is possible for the distance to the gravity center; notably, the simulated response of r(t) in Figure 9 does not violate this constraint as thrusters remain operational during the simulation.

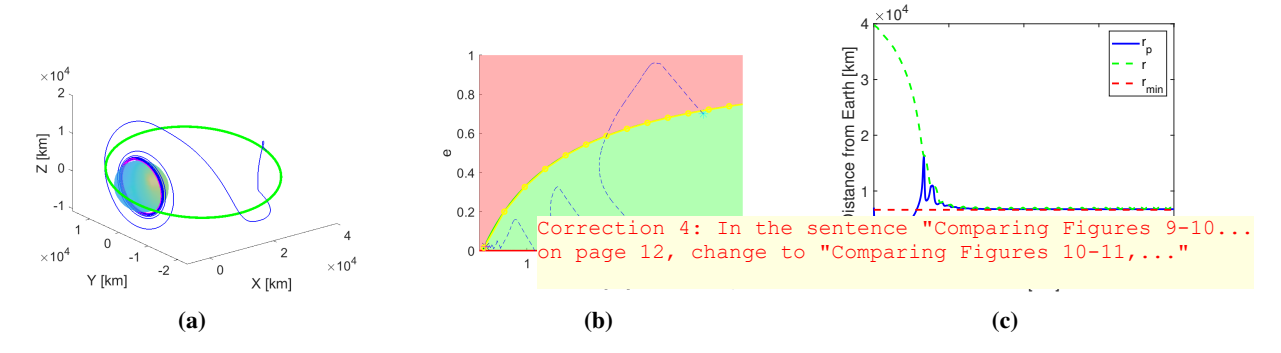


Fig. 9 Orbital transfer from a higher to a lower orbit without CG: (a) Three dimensional trajectory (blue) with initial orbit (green) and target orbit (magenta); (b) Trajectory on a-e plane (dashed) with the region allowed by constraints (32) and (34) shown in green, piecewise linear approximation of (32) shown in yellow*, actual trajectory (blue dashed); (c) The time histories of r_p , r and r_{min} .

Figure 10 illustrates the transfer from the higher orbit to the lower orbit with CG. All the constraints are satisfied. With frozen z_1 and z_2 in (39) at the values of 1, the trajectories are shown in Figure 11. Comparing Figures 9-10 $\overline{z_1}$ and z_2 in the optimization results in faster maneuvers.

Figure 12 illustrates the reverse transfer with CG and governed z_1 and z_2 in (39) from the lower orbit to the higher orbit with (41) and (40) switched. Again, all the constraints are satisfied.

Remark: Numerical issues (fmincon convergence to incorrect points) have precluded us from successfully utilizing MPEC formulation based on (24)-(28), either with or without (10), when applied to the original constraint (32). The numerical difficulties could be expected [15] given that h_1 in (32), which is being maximized in the inner loop, is not a concave function. We leave the application of optimizers specifically developed for bilevel optimization problems, such as [10, 16], to future work.

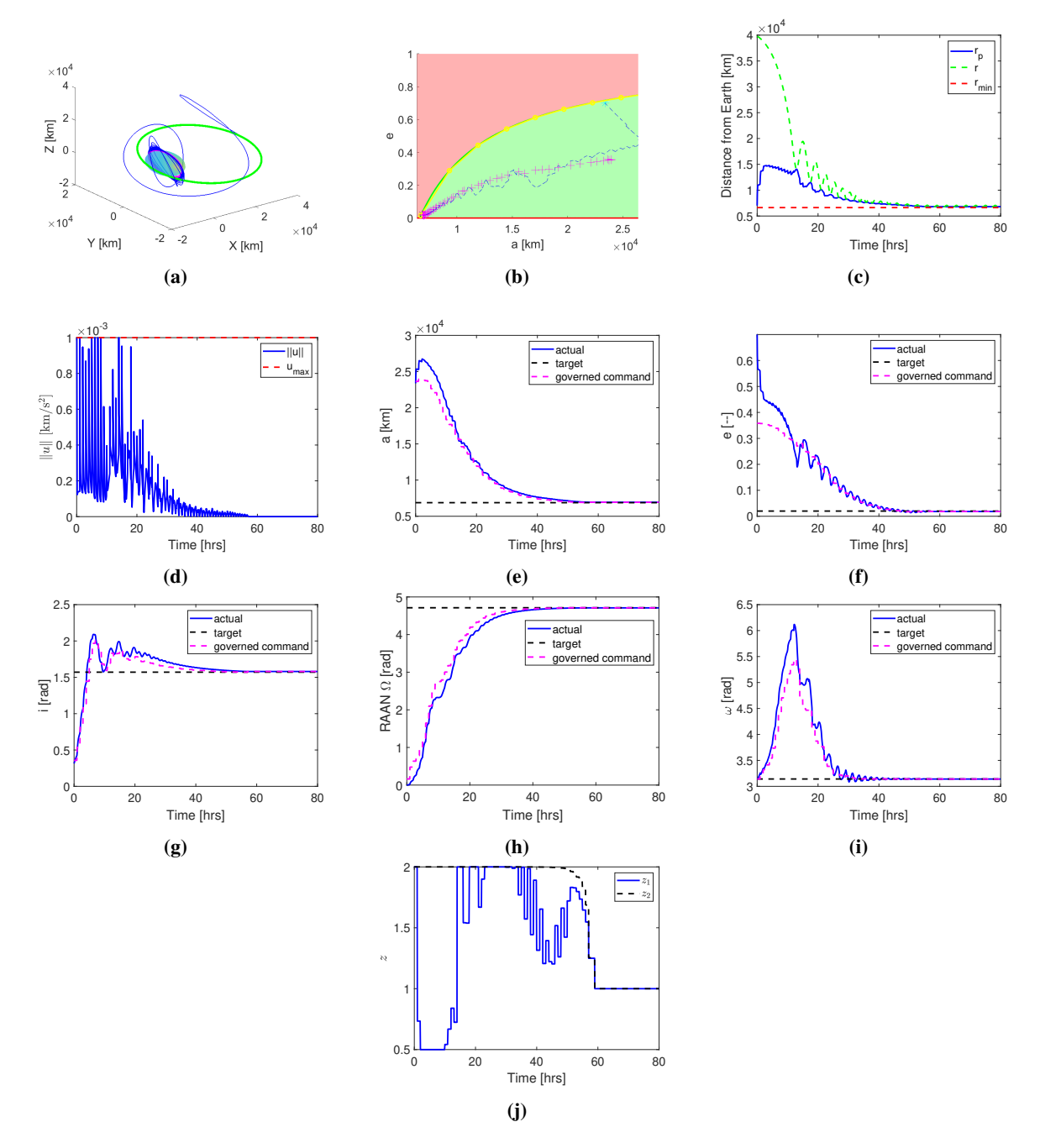


Fig. 10 Orbital transfer from a higher to a lower orbit with CG: (a) Three dimensional trajectory (blue) with initial orbit (green) and target orbit (magenta); (b) Trajectory on a-e plane (dashed) with the region allowed by constraints (32) and (34) shown in green, piecewise linear approximation of (32) shown in yellow, actual trajectory (blue dashed) and v_k (magenta "+"); (c) The time histories of r_p , r and r_{min} ; (d) The time histories of ||u|| and u_{max} ; (e) The time histories of actual (blue, solid), governed command (magenta, dashed) and target semi-major axis (black, dashed); (f) The time histories of actual (blue, solid), governed command (magenta, dashed) and target eccentricity (black, dashed); (g) The time histories of actual (blue, solid), governed command (magenta, dashed) and target inclination (black, dashed); (h) The time histories of actual (blue, solid), governed command (magenta, dashed) and target RAAN (black, dashed); (i) The time histories of actual (blue, solid), governed command (magenta, dashed) and target argument of periapsis (black, dashed); (j) The time histories of multipliers z_1 and z_2 .

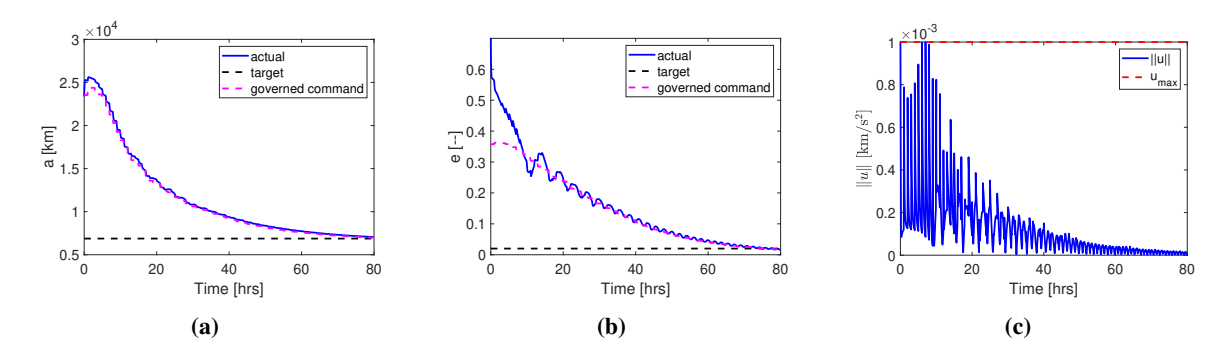


Fig. 11 Orbital transfer from a higher to a lower orbit with CG and with $z_{1,k} = z_{2,k} = 1$: (a) The time histories of actual (blue, solid), governed command (magenta, dashed) and target semi-major axis (black, dashed); (b) The time histories of actual (blue, solid), governed command (magenta, dashed) and target semi-major axis (black, dashed); (c) The time histories of ||u|| and u_{max} .

IX. Conclusion

By using bilevel optimization in the definition of Command Governor (CG) strategy the explicit offline construction of invariant constraint admissible sets could be avoided. This can be advantageous in constrained control problems in which the reference command is multi-dimensional and/or the constraints change online.

We have demonstrated that CG can be implemented in the Gauss Variational Equation (GVE) setting and exploited to enforce constraints during low thrust orbital transfer maneuvers. The approach is based on complementing a quadratic Lyapunov function based controller with CG. The additional flexibility in this approach to optimize the Lyapunov function in the outer loop has also been demonstrated.

Acknowledgments

This research has been supported in part by the National Science Foundation Grant Number CMMI-1904394.

References

- [1] Garone, E., Di Cairano, S., and Kolmanovsky, I., "Reference and command governors for systems with constraints: A survey on theory and applications," *Automatica*, Vol. 75, 2017, pp. 306–328.
- [2] Gilbert, E., and Kolmanovsky, I., "Nonlinear tracking control in the presence of state and control constraints: A generalized reference governor," *Automatica*, Vol. 38, No. 12, 2002, pp. 2063–2073.
- [3] Weiss, A., Baldwin, M., Erwin, R. S., and Kolmanovsky, I., "Model predictive control for spacecraft rendezvous and docking: Strategies for handling constraints and case studies," *IEEE Transactions on Control Systems Technology*, Vol. 23, No. 4, 2015, pp. 1638–1647.
- [4] Dempe, S., and Zemkoho, A. B., "The bilevel programming problem: Reformulations, constraint qualifications and optimality conditions," *Mathematical Programming*, Vol. 138, 2013, pp. 447–473.
- [5] Gilbert, E. G., and Kolmanovsky, I. V., "Set-point control of nonlinear systems with state and control constraints: A Lyapunov-function, Reference-Governor approach," *Proceedings of the 38th IEEE Conference on Decision and Control (Cat. No. 99CH36304)*, Vol. 3, IEEE, 1999, pp. 2507–2512.
- [6] Garone, E., and Kolmanovsky, I., "Command governors with inexact optimization and without invariance," *Journal of Guidance, Control, and Dynamics*, Vol. 45, No. 8, 2022, pp. 1523–1528.
- [7] Garone, E., Nicotra, M., and Ntogramatzidis, L., "Explicit reference governor for linear systems," *International Journal of Control*, Vol. 91, No. 6, 2018, pp. 1415–1430.
- [8] Kim, Y., Leyffer, S., and Munson, T., "MPEC methods for bilevel optimization problems," *Bilevel Optimization: Advances and Next Challenges*, 2020, pp. 335–360.
- [9] Sinha, A., Malo, P., and Deb, K., "A review on bilevel optimization: From classical to evolutionary approaches and applications," *IEEE Transactions on Evolutionary Computation*, Vol. 22, No. 2, 2017, pp. 276–295.

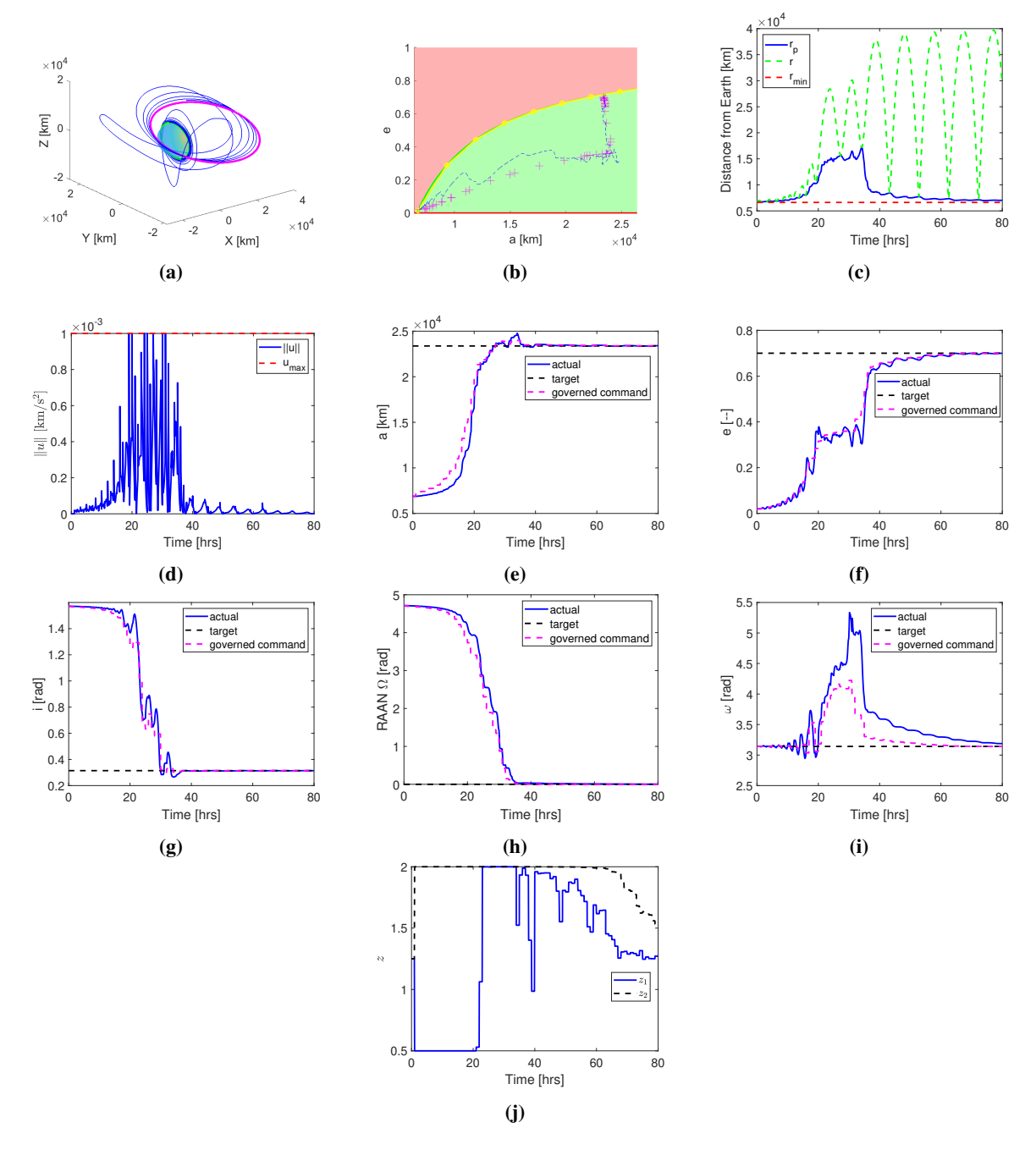


Fig. 12 Orbital transfer from a lower to a higher orbit with CG: (a) Three dimensional trajectory (blue) with initial orbit (green) and target orbit (magenta); (b) Trajectory on a-e plane (dashed) with the region allowed by constraints (32) and (34) shown in green, piecewise linear approximation of (32) shown in yellow, actual trajectory (blue dashed) and v_k (magenta "+"); (c) The time histories of r_p , r and r_{min} ; (d) The time histories of ||u|| and u_{max} ; (e) The time histories of actual (blue, solid), governed command (magenta, dashed) and target semi-major axis (black, dashed); (f) The time histories of actual (blue, solid), governed command (magenta, dashed) and target inclination (black, dashed); (h) The time histories of actual (blue, solid), governed command (magenta, dashed) and target RAAN (black, dashed); (i) The time histories of actual (blue, solid), governed command (magenta, dashed) and target argument of periapsis (black, dashed); (j) The time histories of multipliers z_1 and z_2 .

- [10] Zhou, S., and Zemkoho, A. B., "BiOpt: Bilevel optimization toolboxes," Tech. rep., https://biopt. github. io/files/menu-of-BiOpt. pdf, 2021.
- [11] Bagirov, A., Karmitsa, N., and Mäkelä, M. M., *Introduction to Nonsmooth Optimization: Theory, practice and software*, Vol. 12, Springer, 2014.
- [12] Gurfil, P., and Seidelmann, P. K., Celestial Mechanics and Astrodynamics: Theory and Practice, Vol. 436, Springer, 2016.
- [13] Battin, R. H., An Introduction to the Mathematics and Methods of Astrodynamics, AIAA, 1999.
- [14] Kolmanovsky, I., and Sun, J., "Parameter governors for discrete-time nonlinear systems with pointwise-in-time state and control constraints," *Automatica*, Vol. 42, No. 5, 2006, pp. 841–848.
- [15] Dempe, S., "Bilevel optimization: Theory, algorithms, applications and a bibliography," *Bilevel Optimization: Advances and Next Challenges*, 2020, pp. 581–672.
- [16] Zhou, S., Zemkoho, A. B., and Tin, A., "BOLIB: Bilevel Optimization LIBrary of test problems," *Bilevel Optimization: Advances and Next Challenges*, 2020, pp. 563–580.